SINTEF
PROCEEDINGS 6

14th International Conference on CFD in
Oil & Gas, Metallurgical and Process Industries
SINTEF, Trondheim, Norway, October 12–14, 2020

Proceedings from the 14th International Conference on CFD in Oil & Gas, Metallurgical and Process Industries

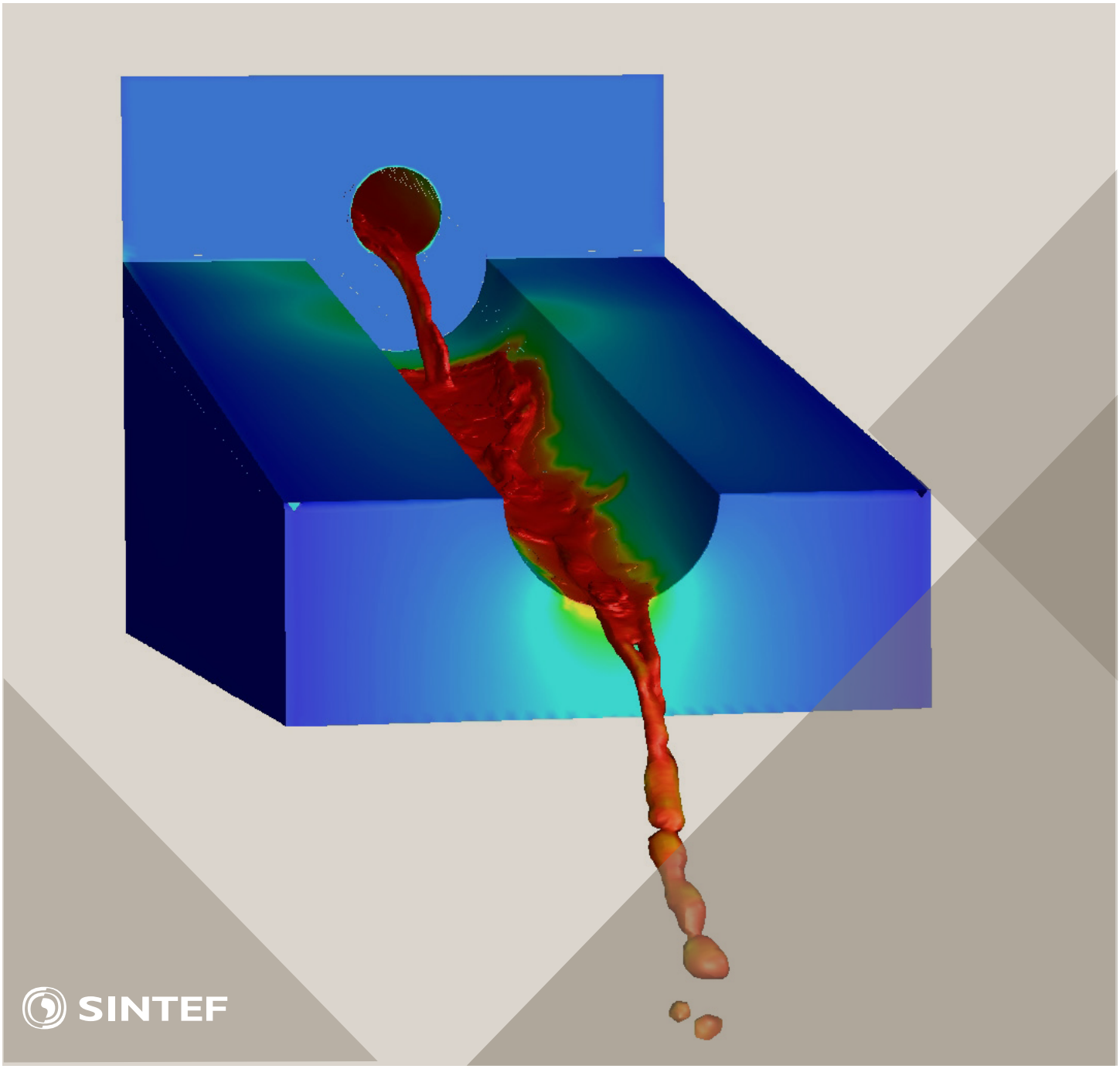

SINTEF Proceedings

Editors:
Jan Erik Olsen, Jan Hendrik Cloete and Stein Tore Johansen

Proceedings from the 14th International Conference on CFD in Oil & Gas, Metallurgical and Process Industries

SINTEF, Trondheim, Norway
October 12–14, 2020

SINTEF Academic Press

SINTEF Proceedings 6
Editors: Jan Erik Olsen, Jan Hendrik Cloete and Stein Tore Johansen

Proceedings from the 14th International Conference on CFD in Oil & Gas, Metallurgical and Process Industries, SINTEF, Trondheim, Norway, October 12–14, 2020

Keywords:
CFD, fluid dynamics, modelling

Cover illustration: Tapping of metal by Jan Erik Olsen

ISSN 2387-4295 (online)
ISBN 978-82-536-1684-1 (pdf)

© 2020 The Authors. Published by SINTEF Academic Press.
SINTEF has the right to publish the conference contributions in this publication.
This is an open access publication under the CC BY license
https://creativecommons.org/licenses/by/4.0/

SINTEF Academic Press
Address: Børrestuveien 3
PO Box 124 Blindern
N-0314 OSLO
Tel: +47 40 00 51 00

www.sintef.no/community
www.sintefbok.no

SINTEF Proceedings
SINTEF Proceedings is a serial publication for peer-reviewed conference proceedings on a variety of scientific topics.
The processes of peer-reviewing of papers published in SINTEF Proceedings are administered by the conference organizers and proceedings editors. Detailed procedures will vary according to custom and practice in each scientific community.

14th International Conference on CFD in Oil & Gas, Metallurgical and Process Industries
SINTEF, Trondheim, NORWAY
October 12-14, 2020

MODELLING OF WAX DEPOSITION IN OIL PIPES: A DISPERSED MULTIPHASE TURBULENT FLOW APPROACH

Federico MUNICCHI[1*], **Ismail El MELLAS**[2], **Matteo ICARDI**[1], **Mirco MAGNINI**[2]
[1]School of Mathematical Sciences, University of Nottingham, Nottingham NG72RD, UK
[2]School of Engineering, University of Nottingham, Nottingham NG72RD, UK
* E-mail: federico.municchi@nottingham.ac.uk

ABSTRACT
Crude oils are complex mixtures of hydrocarbons including high molecular weight paraffin waxes. When a "waxy" crude oil flows through a cold pipeline whose temperature is below the wax appearance temperature, e.g. in subsea transportation systems, heavy paraffins separate and deposit on the pipe walls. The available prediction methods for wax deposition are essentially empiric, particularly regarding the description of the fouling deposition and removal processes, which depend on the fluid dynamic interaction between the deposit layer and the bulk flow. In this work, we present a novel theoretical and numerical model for predicting wax deposition in oil pipes and, more generally, coagulation/deposition processes for a wide range of applications. Unlike other models existing in literature, which are mostly based on a separated two-fluid description of the oil/wax-oil flow and phase-change represented as a deposition process, our model is based on a mixture description, where wax is considered as a suspended phase immersed in crude-oil. Coagulation and dissolution phenomena are modelled with an associated first order kinetic reaction which allows to study arbitrarily complex geometries. Wax ageing (hardening) is solved with a dynamic equation for the viscosity. We show how this model can be implemented in the open-source C++ library OpenFOAM and we present key results for deposition in a variety of pipe shapes.

Keywords: CFD, multiphase flows, deposition, asphaltenes .

NOMENCLATURE

Greek Symbols
ϕ Solid volume fraction, $[-]$
ν Kinematic viscosity, $[m^2/s]$
α Heat diffusivity, $[m^2/s]$
ϕ_m Maximum solid volume fraction, $[-]$
τ_s Settling time, $[s]$
τ_c Characteristic coagulation time, $[s]$
τ_d Characteristic dissolution time, $[s]$
β Expansion factor, $[K^{-1}]$
θ Hardening time, $[s^{-1}]$
σ Shear-breaking time scale, $[s]$
$\dot{\gamma}$ Strain rate, $[s^{-1}]$
λ Ageing factor, $[-]$

Latin Symbols
$\boldsymbol{u}$ Velocity, $[m/s]$.
p Pressure, $m^2/s^2]$.
T Temperature, $[K]$.
c Molar concentration, $[-]$.
D_c Diffusion coefficient of c, $[m^2/s]$.
$\dot{S}$ Deposition rate, s^{-1}.

Sub/superscripts
s Solid.
o Oil.
t Turbulent.
eq Equilibrium .
ref Reference .
mix Mixture .

INTRODUCTION
Wax deposition represents a significant flow assurance problem for the oil and gas industry because it can lead to restriction and then blockage of oil reservoir formations, pipelines, and process equipment. Crude oil is a complex mixture of saturates (paraffin/waxes), aromatics, naphthenes, asphaltenes, and resins. Among these components, high molecular weight paraffin (waxes) and asphaltenes are typically the main cause for production and transportation problems in subsea pipeline systems. At reservoir temperatures ($70 - 150\,^{\circ}\mathrm{C}$) and pressures ($50 - 100\,\mathrm{MPa}$), wax molecules can be found dissolved in the crude oil. However, during transportation crude oil flows through pipelines located in cooler environments, e.g. in sub-sea pipelines resting on the ocean floor at temperatures of $4\,^{\circ}\mathrm{C}$. Owing to the thermal losses to the surroundings, the temperature of oil can quickly decrease below the cloud point temperature (or wax appearance temperature, WAT). The solubility of wax decreases drastically as the temperature decreases, and wax molecules start to precipitate out of the crude oil (Singh *et al.*, 2000). Waxes have long molecular chains and they usually form stable wax crystals and a solid network. The network trapped liquid is like a vector for further diffusion of heavier hydrocarbons molecules that appear with the counter diffusion of the trapped oil out of the deposit. A large number of mechanisms have been suggested to be responsible for the deposition of solids from waxy crude oil mixtures, including molecular diffusion, Soret diffusion, Brownian motion, shear dispersion, and gravity settling (Burger *et al.*, 1981; Azevedo and Teixeira, 2003). Molecular diffusion has been often regarded as the main deposition mechanism and, accordingly, the deposition rate is calculated as proportional to the concentration gradient at the wall (Burger *et al.*, 1981; Svendsen, 1993). Many different

models to predict the build-up of the deposit layer on the cold wall of a pipeline have been proposed, with different levels of sophistication, see Magnini and Matar (2019) for a recent review. These models are mainly one-dimensional, and predict the thickness of the wax layer as a function of time along the pipeline, based on a balance of deposition and removal terms. Deposition is usually modelled following molecular diffusion, and therefore calculating the deposition rate according to the gradient of the fluid temperature at the wall. The latter is reconstructed according to simplified fluid dynamics model of the flow in the pipe, assuming laminar or turbulent velocity profiles (Svendsen, 1993; Ramirez-Jaramillo *et al.*, 2001; Singh *et al.*, 2001). The deposit removal is due to the shear exerted by the fluid and is typically modelled empirically, by means of a negative source term with attempts to correlate this to wall shear, deposit thickness or time (Correra *et al.*, 2007; Eskin *et al.*, 2013; Ramirez-Jaramillo *et al.*, 2004; Solaimany Nazar *et al.*, 2005). In particular, time is an important factor in the build-up of the deposit because it makes the deposit harder, a phenomenon known as "ageing". Although one-dimensional models have the great advantage of being little time-consuming to run, their drawback is that the mechanisms of deposition and removal are poorly linked to the actual fluid mechanics and heat transfer characteristics of the flow. Direct numerical simulations promise to be a very effective tool to investigate the fundamental mass, momentum and energy exchanges leading to wax deposition and removal, however the only approach published so far (Magnini and Matar, 2019) utilised interface-resolving simulations using a time-explicit Volume-Of-Fluid method, which dramatically limits the temporal duration of the flow that can be simulated.

This work represents a step forward in the direction of direct numerical simulations of the crude-oil flow and resulting wax deposition, but using a more efficient and less time-consuming technique to deal with the different phases present in the flow. Furthermore, we introduce a novel rheological model for the viscosity of the deposited mass which accounts for ageing effects upon solution of a transport equation for the ageing time.

MODEL DESCRIPTION

In our model, we employ a mixture model similar to the suspension balance model (Nott and Brady, 1994) to describe the suspension of solid particles of coagulated wax in the suspending crude oil as an effective fluid. Therefore, we introduce a phase volume fraction ϕ representing the volume occupied by the solid particles with respect to the total volume of the mixture, that we assume incompressible.

Momentum transport

The mixture velocity is then defined as:

$$\boldsymbol{u} = \phi \boldsymbol{u}_s + (1-\phi)\boldsymbol{u}_o \,, \tag{1}$$

where $\boldsymbol{u}_s$ and $\boldsymbol{u}_o$ are the solid and crude oil velocities respectively. Then, the momentum conservation equation for the whole mixture reads:

$$\frac{\partial \boldsymbol{u}}{\partial t} + \boldsymbol{\nabla}\cdot(\boldsymbol{u}\boldsymbol{u}) = -\boldsymbol{\nabla} p + \boldsymbol{\nabla}\cdot\left[\nu_{\text{mix}}\left(\boldsymbol{\nabla}\boldsymbol{u} + \boldsymbol{\nabla}^T\boldsymbol{u}\right)\right] \,, \tag{2}$$

together with the incompressibility condition;

$$\boldsymbol{\nabla}\cdot\boldsymbol{u} = 0 \,. \tag{3}$$

Notice that in equation 2 we denoted the pressure field as p and the mixture kinematic viscosity as ν_{mix}. Hence, equations 2 and 3 provide a global description of the effective fluid, where phase-specific forces and fluxes like drag and gravity currents cancel out. The only term that really plays a role in representing the multiphase system is the mixture density ν_{mix}, which we express as a linear combination of turbulent and suspension contribution:

$$\nu_{\text{mix}} = \nu_t + \nu_s \tag{4}$$

where ν_t is the usual turbulent viscosity and ν_s is the added viscosity due to the suspended phase. In this work, we employ a RANS standard κ–ϵ model (Launder and Spalding, 1974) to model the turbulence. A key feature of asphaltenes is their tendency to agglomerate resulting in the formation of solid structures that becomes more impermeable with time. This process is called "ageing", and it will be discussed in a later section.

Concerning the solid phase, we are not solving a separate momentum transport equation. Instead, we assume that the settling time of the particles is sufficiently small that its velocity can be directly computed from the mixture velocity, such that the slip velocity is given by (Ferry *et al.*, 2003):

$$\boldsymbol{u}_{\text{slip}} = \tau_s \left(\frac{\partial \boldsymbol{u}}{\partial t} + \boldsymbol{u}\cdot\boldsymbol{\nabla}\boldsymbol{u}\right) \,. \tag{5}$$

Notice that equation 5 is only valid under the assumption that no gravitational forces are present, and its overall effect is that of relaxing $\boldsymbol{u}_{\text{slip}}$ to zero. Consequently, our model considers only small deviations between the velocities of the two phases.

Within this work, we will therefore assume that the oil and solid velocities can be computed from:

$$\boldsymbol{u}_s = \boldsymbol{u}_o + \boldsymbol{u}_{\text{slip}} \,, \tag{6}$$

where $\boldsymbol{u}_{\text{slip}}$ is a small deviation. Hence, the mixture velocity is given by:

$$\boldsymbol{u} = \boldsymbol{u}_s - (1-\phi)\boldsymbol{u}_{\text{slip}} = \boldsymbol{u}_o + \phi\boldsymbol{u}_{\text{slip}} \,. \tag{7}$$

Rearranging leads to the expressions:

$$\boldsymbol{u}_s = \boldsymbol{u} + (1-\phi)\boldsymbol{u}_{\text{slip}} \,, \tag{8}$$

$$\boldsymbol{u}_o = \boldsymbol{u} - \phi\boldsymbol{u}_{\text{slip}} \,. \tag{9}$$

Species transport and thermodynamics

We assume that the transport properties are not depending on the temperature T and that the suspension flow is in thermal equilibrium (i.e., the temperature of the solid and the liquid phases are approximately the same) as is often the case in non-Brownian suspensions (Dbouk, 2018). Thus, we can write the transport equation for the temperature as:

$$\frac{\partial T}{\partial t} + \boldsymbol{u}\cdot\boldsymbol{\nabla}T = \alpha\nabla^2 T \,, \tag{10}$$

Where α is the heat diffusivity of the mixture, which we assume equal to that of crude oil.

As a consequence of mass conservation, an advection equation is employed to evolve the solid volume concentration ϕ:

$$\frac{\partial \phi}{\partial t} + \boldsymbol{\nabla}\cdot(\boldsymbol{u}_s\phi) = \dot{S}(1-\phi) \,, \tag{11}$$

where $\dot{S}$ is the creation-destruction term due to coagulation or dissolution and it is a function of the temperature T and

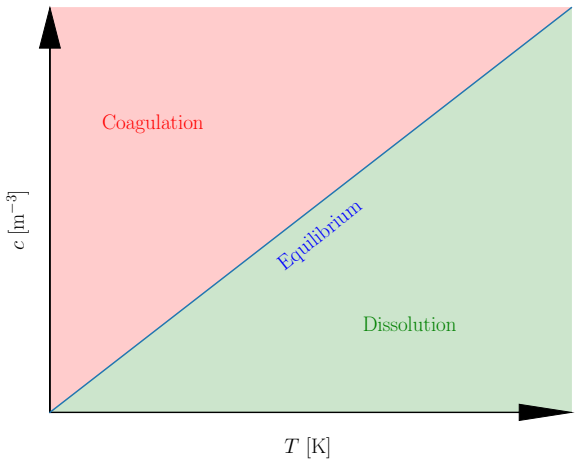

Figure 1: Schematic representation of the equilibrium change as a function of temperature and concentration.

the concentration of asphaltenes c in the crude oil. At the heart of our model, there is the expression for $\dot{S}$:

$$\dot{S}(c,T) = \begin{cases} \dfrac{1}{\tau_c}\left(c - c_{eq}(T)\right) & \text{if } c > c_{eq}(T) \\ \dfrac{\phi}{\tau_d}\left(c - c_{eq}(T)\right) & \text{if } c < c_{eq}(T) \end{cases} \tag{12}$$

where c is the molar concentration of asphaltenes in the crude oil, while τ_d and τ_r are the characteristic time scales associated with coagulation and dissolution. For simplicity, we also assume that the equilibrium concentration can be represented as a linear function of the temperature:

$$c_{\text{eq}} = c_{\text{ref}} + \beta\left(T - T_{\text{ref}}\right), \tag{13}$$

where the subscript ref indicates reference quantities.
As shown in Figure 1, our mathematical model predicts that coagulation occurs at lower temperatures, while the asphaltenes tend to dissolve into the fluid phase at higher temperatures.
Clearly, our model requires the solution of the transport equation for the molar concentration c in the crude oil:

$$\frac{\partial\left(1-\phi\right)c}{\partial t} + \boldsymbol{\nabla}\cdot\left[\left(1-\phi\right)\boldsymbol{u}_o c\right] = \boldsymbol{\nabla}\cdot\left[\left(1-\phi\right)D_c\boldsymbol{\nabla}c\right] - \dot{S}\left(1-\phi\right), \tag{14}$$

where D_c is the diffusion coefficient of asphaltenes in crude oil. Notice that summing Equations 14 and 11 the source term disappears since the total mass transferred between the phases is conserved by our model.

Deposit ageing and hardening

It is well known that wax deposits exhibit non local (in time) phenomena that lead to dramatic changes in their material properties (Hewitt, 2015). The most noticeable of these is hardening. The thermal gradient across the walls and the deposit layer result in an internal mass flux which leads to a continuous increase of the solid particles content. This leads to a significant hardening of the sub layer with time, i.e. the aging process.

Following the approach of Sileri *et al.* (2011), we model the viscosity of the solid phase as the product of the classic Maron-Pierce viscosity for suspensions of spheres (Maron and Pierce, 1956) with an ageing term (Roussel N, 2004):

$$\nu_s = \nu\left(\frac{\phi_m}{\phi_m - \phi}\right)^2\left(1 + \lambda\phi\right), \tag{15}$$

where ν is the laminar kinematic viscosity of crude oil, ϕ_m is the maximum packing fraction of the solid phase (set equal to 1). λ is a structure parameter that describes the iteration of network of wax crystals.
The structure parameter contains the flow history and it is obtained from the rivalry of two opposite behaviours, a structuration process where the crystals are spontaneously formed and a de-structuration process which causes a continued removal of the crystals network.
In our work, we propose a transport equation for the structure parameter:

$$\frac{\partial\lambda}{\partial t} + \boldsymbol{\nabla}\cdot\left(\phi\boldsymbol{u}_s\lambda\right) = \phi\left(\frac{1}{\theta} - \sigma\dot{\gamma}\lambda\right). \tag{16}$$

The last term in equation 16 follows the expression proposed by Huynh *et al.* (2005) and Coussot *et al.* (2005), where the parameters σ and θ control the generation and destruction of λ. Equation 16 allows to properly model the ageing process in a fluid domain, where the information regarding the residence time of the particulate is transported by the mixture.

Numerical solution

We developed an application in the open-source finite volume library OpenFOAM® to solve the governing equations of our model. We employ a PIMPLE algorithm (fundamentally a fixed point iteration) to couple the seven transport equations in a segregated manner. For each time step, the application performs the operations below:

Numerical procedure adopted to solve the model equations:

1. Update the viscosity ν_{mix} using equation 4;
2. Assemble the velocity matrix and solve for p using the PISO algorithm (Issa, 1986);
3. Solve for T using equation 10;
4. Update c_{eq} (equation 13) and compute $\dot{S}$ (equation 12) using the actual value of c;
5. Update $\boldsymbol{u}_{\text{slip}}$ using equation 5 and solve for ϕ using equation 11;
6. Solve for c using equation 14;
7. Solve for λ using equation 16;
8. Proceed to the next time step if the convergence criteria are satisfied. Otherwise, repeat from point 1.

Convergence criteria are specified as thresholds on the residuals for each field equal to 10^{-5}. We found this procedure capable of producing stable solutions in a short time and without convergence issues. Laplace operators are discretised using linear schemes, while divergences are discretised using linear upwind schemes. One noticeable exception is

the divergence in the equation for ϕ that we discretised using a van Leer scheme bounded between zero and one to improve the roboustness of the algorithm. All time derivatives where discretised using a second order backward finite difference scheme.

RESULTS

In order to illustrate the usage of the proposed model, we will first calibrate the values of τ_c and τ_d using the experiments of Singh *et al.* (2017). Subsequently, we show how the model can be applied to study the dynamics of deposition in oil pipes. Finally, we will investigate the effects of ageing.
In all simulations, the computational domain consists in a cylinder with diameter D (40 cells) and length L (50 cells). Due to the symmetry of the problem (we assume that gravity does not play a significant role) we employ a structured axial-symmetric grid to represent the cylindrical pipe. In order to resolve the boundary layer and predicting the onset of wall deposition, we graded the mesh spacing such that the grid is finer at the pipe wall.

Boundary conditions

We impose a fixed velocity and temperature, at the inlet, where we also set volume concentration of asphaltenes to 1 and ϕ to zero. We assume fully developed fields (zero gradient) at the outlet. At the wall, we employ a fixed temperature condition and a no slip velocity condition, while a zero gradient condition is imposed for the concentration of asphalthenes. The material properties employed in this work are listed in Table 1.

Table 1: List of material properties employed

Property	Symbol	Units	Value
Kinematic viscosity	ν	[m^2/s]	0.01051
Diffusion coefficient	D_c	[m^2/s]	10^{-7}
Reference temperature	T_{ref}	[K]	319
Initial temperature	T_i	[K]	293
Particle settling time	τ_s	[s]	10^{-32}
Maximum solid volume fraction	ϕ_m	[-]	1
Characteristic coagulation time	τ_c	[s]	$5 \cdot 10^2$
Characteristic dissolution time	τ_d	[s]	10^{-3}
Thermal diffusivity	α	[m^2/s]	0.134
Expansion factor	β	[1/ K]	0.65
Viscosity destruction term	σ	[-]	0.65
Viscosity hardening coefficient	θ	[s]	0.5

Calibration of the coagulation and dissolution rates

Table 2: Initial conditions and parameters for the calibration against Singh *et al.* (2017)

D $[m]$	$\boldsymbol{u}_{in}$ $[^m/_s]$	T_{in} $[K]$	T_w $[K]$	σ $[^1/_s]$	θ $[-]$
0.0165	1.83	298	289	0	0

To obtain appropriate values for the coagulation and dissolution rates, we investigate a wide range of values of τ_c and τ_d in the absence of ageing. The predicted deposition rate is compared against results from Singh *et al.* (2017) to find the values that give the best matching. Notice that assumption of absence of ageing effects is only justified if we look at the first seconds of the deposition process. Results from Singh *et al.* (2017) show that the deposition rate approaches an asymptotic linear trend after an initial transient. We therefore calibrate τ_c and τ_d to closely match that value, as the nonlinear transient would require a model with multiple time scales, like that proposed by Municchi and Icardi (2020). Here, we are interested in capturing the linear mode only.

In Singh *et al.* (2017), a wax deposition experiment was conducted using a Garden Banks condensate as operating fluid, circulated in turbulent flow conditions. All the relevant parameters they employed are collected in Table 2.

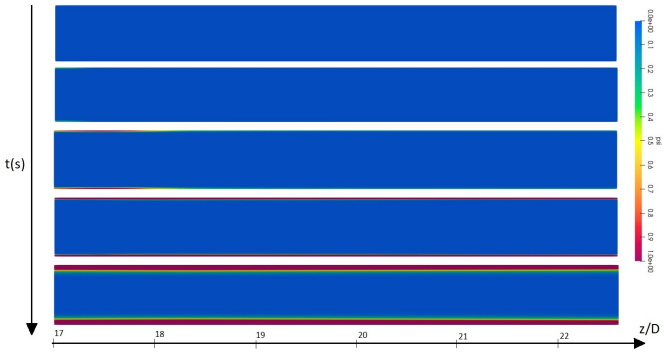

Figure 2: Evolution in time of the deposition

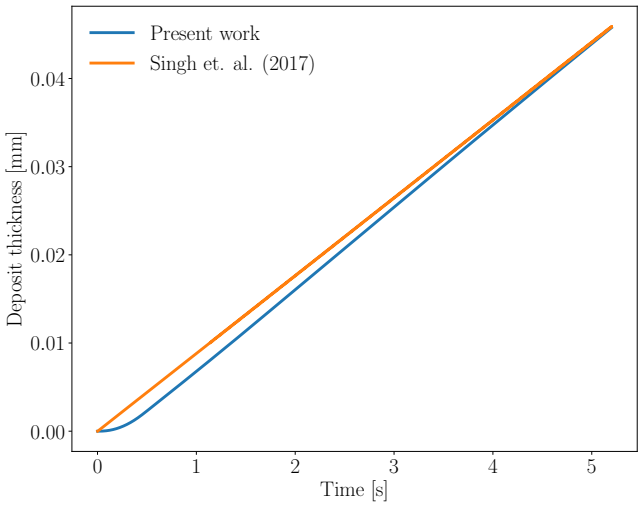

Figure 3: Deposition rate as predicted by our simulation and measured by Singh *et al.* (2017)

Figure 2 shows the evolution in time of the deposit, represented by the field ϕ. We notice that a layer of substantial deposit gradually starts to agglomerate, and attaches to the wall as a consequence of the radial temperature gradient. Therefore, the model predicts the correct physical behaviour of the system.
The dynamics of the model works as follows: particles are forming based on the difference between c and c_{eq}, which is a function of the temperature. Once formed, the particles alter the fluid viscosity increasing the resistance to the flow. Large clusters of particles forming in the middle of the channel will be advected downstream, while layers forming at the wall will continue to grow as they reduce the already small velocity field in that region. On the time-scale of the layer growth, one can observe that a sharp interface is forming between the almost clear fluid in the bulk and the solid formation growing from the wall.
The rate of mass deposition $\dot{S}$ is negligible (compared to the advective flux) everywhere except at the interface between the two phases. After a time $t = 10s$, the average thickness of the deposit layer is approximately persistent, and the flow reaches a steady-state. Notice that this would be different if we included the effect of ageing in this simulation.

The reduction in the cross section of the pipe causes the flow field to accelerate up to five times the inlet velocity. Another phenomenon that occurs, is the formation of small waves when the deposit film becomes sufficiently thick, and can therefore detach from the fluid downstream. However, the flow within the travelling waves exhibits a substantially larger speed depending on the height of the wave, and it may reach values as high as $0.15m/s$, with the waves "surfing" over an almost sluggish layer of deposit. This is a numerical artifact and not a physical phenomenon (Magnini and Matar, 2019). The growth rate can be defined as the time variation of the deposit height h in the radial direction $\hat{r}$:

$$\dot{h} = (\boldsymbol{u} \cdot \hat{r})(\boldsymbol{\nabla}\phi \cdot \hat{r}). \tag{17}$$

Figure 3 shows the average thickness of wax long the pipe in time, demonstrating that the model is capable to obtain good agreement with experimental results.

Parametric Study

We now explore a limited range of parameters and discuss their repercussions on the wax deposition and detach process. We investigate the effects of the inlet average crude oil velocity, channel diameter, ageing process and inlet crude oil temperature. Table 3 shows the different scenarios we explored.

Table 3: List of operation conditions we probed in the parametric study

Case	$D\ [m]$	$\boldsymbol{u}_{\text{in}}\ [^m/_s]$	$T_{\text{in}}\ [K]$	$T_{\text{w}}\ [K]$	$\sigma\ [^1/_s]$	$\theta\ [-]$
1	0.0165	0.092	298	289	0	0
2	0.0165	3.66	298	289	0	0
3	0.001	1.83	298	289	0	0
4	0.1	1.83	298	289	0	0
7	0.0165	1.83	298	289	0.1	0.1
8	0.0165	1.83	298	289	1	0.001

Effect of the velocity field

Figure 4 shows that during the early stage of wax deposition the deposition rate decreases with the Reynolds number because of the consequent increase in the Péclet number. Higher velocity fields also increase detachment and transport downstream, leading to the formation of a thinner layer of deposit.

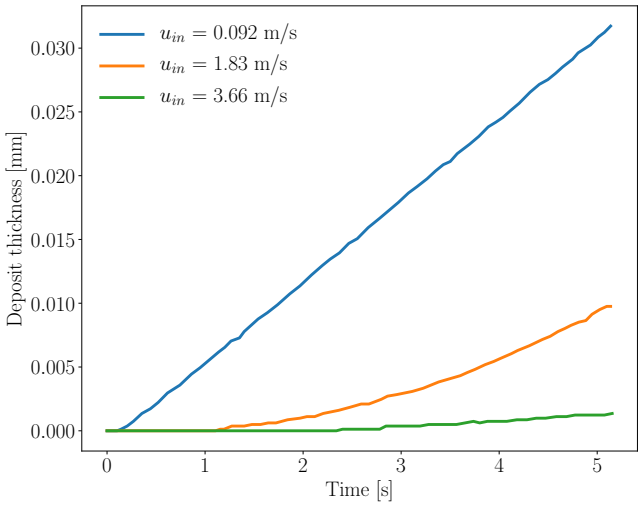

Figure 4: Time evolution of the deposit thickness for different values of the inlet velocity.

Effect of the pipe diameter

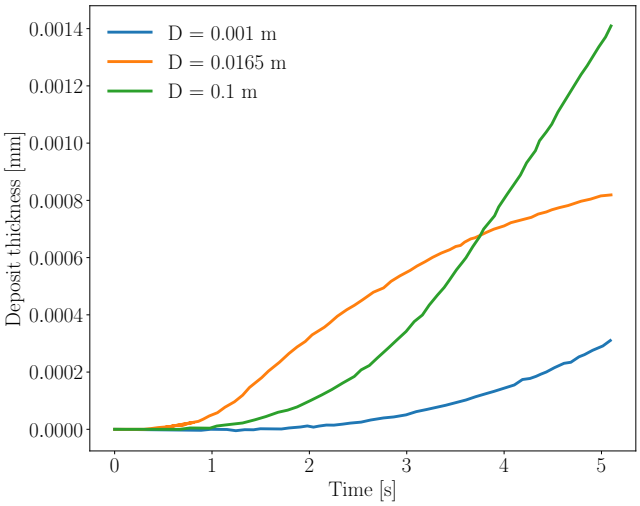

Figure 5: Time evolution of the deposit thickness for different values of the pipe diameter (cases 2, 3, and 4).

In order to compare the absolute values of the film thickness at different diameters, we rescale the film thickness with respect to the pipe radius. The diameter of the pipe appears to have a significant influence on the deposition dynamics as shown in Figure 5. In fact, a steady state flow, characterised by a constant growth of the deposit layer, is reached more quickly in larger pipes. In case 3 the models for asphaltene deposition in the reservoir pores becomes more relevant, and should include capillary forces (Magnini and Matar, 2019; Lawal *et al.*, 2012) due to the low impact of the advective transport compared to viscous forces.

Effect of the ageing λ

We now investigate the effects of ageing processes on the mixture rheology. We simulate two configurations of σ and θ, using parameters similar to those in Sileri *et al.* (2011) for the asphaltene. Figure 6 shows that ageing phenomena exert a strong influence on the flow behavior, affecting the motion of the sub-layer significantly. After a time $t = 50s$ such influence becomes more incisive.

CONCLUSIONS AND OUTLOOK

We proposed a new mathematical model for the coagulation and dissolution of asphaltenes in crude oil, and presented a stable numerical approach to its solution.

Our model possesses several novel aspects as (i) attempts to describe the problem of deposition through coagulation/dissolution using a kinetic approach rather than using a diffusive flux approach and (ii) implements a full non-equilibrium model for the transport of the structure parameter. This allows to model the effects of aging and hardening in complex flows, where transport phenomena are significant.

We demonstrated that the model can be calibrated to obtain reasonably accurate results, and that it is able to provide physically sound predictions in a number of configurations. Specifically, we illustrated how our model can be employed to analyse different scenarios in oil pipes.

Future works will require a combination of experimental and theoretical approaches to identify proper values for the free parameters that are present in the model. Furthermore, ex-

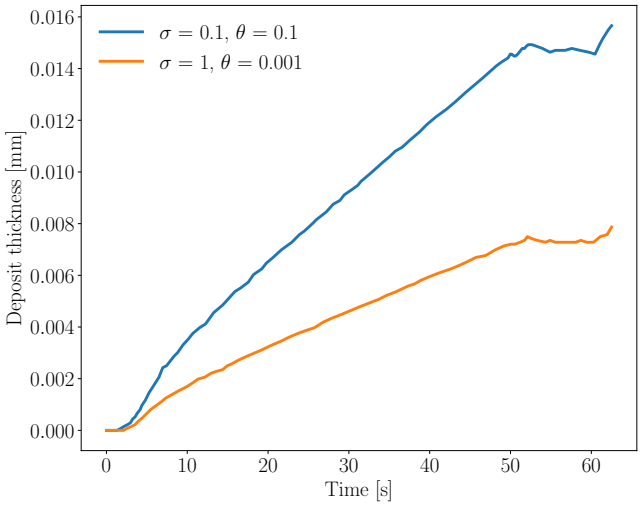

Figure 6: Time evolution of the deposit thickness for different values of the parameters in the transport equation λ.

tension to precipitation applications with gravity and variable density is ongoing.

However, the lack of field data regarding the coagulation and dissolution rates pose significant limits to the current methodology, which strongly relies on calibration.

REFERENCES

AZEVEDO, L.F.A. and TEIXEIRA, A.M. (2003). "A critical review of the modeling of wax deposition mechanisms". *Petrol. Sci. Technol.*, **21**, 393–408.

BURGER, E.D., PERKINS, T.K. and STRIEGLER, J.H. (1981). "Studies of wax deposition in the trans alaska pipeline". *J. Petrol. Technol.*, **33**, 1075–1086.

CORRERA, S., FASANO, A., FUSI, L. and MERINO-GARCIA, D. (2007). "Calculating deposit formation in the pipelining of waxy crude oils". *Meccanica*, **42**, 149–165.

COUSSOT, P., ROUSSEL, N., JARNY, S. and CHANSON, H. (2005). "Continuous or catastrophic solid–liquid transition in jammed systems". *Physics of Fluids*, **17(1)**, 011704. URL `http://aip.scitation.org/doi/10.1063/1.1823531`.

DBOUK, T. (2018). "Heat transfer and shear-induced migration in dense non-Brownian suspension flows: Modelling and simulation". *Journal of Fluid Mechanics*, **840**, 432–454.

ESKIN, D., RATULOWSKI, J. and AKBARZADEH (2013). "A model of wax deposit layer formation". *Chem. Eng. Sci.*, **97**, 311–319.

FERRY, J., RANI, S.L. and BALACHANDAR, S. (2003). "A locally implicit improvement of the equilibrium Eulerian method". *International Journal of Multiphase Flow*, **29(6)**, 869–891.

HEWITT, G. F.AND COLETTI, F. (2015). "Crude oil fouling". *Gulf Professional Publishing*.

HUYNH, H.T., ROUSSEL, N. and COUSSOT, P. (2005). "Aging and free surface flow of a thixotropic fluid". *Physics of Fluids*, **17(3)**, 033101. URL `http://aip.scitation.org/doi/10.1063/1.1844911`.

ISSA, R. (1986). "Solution of the implicitly discretised fluid flow equations by operator-splitting". *Journal of Computational Physics*, **62(1)**, 40–65. URL `https://linkinghub.elsevier.com/retrieve/pii/0021999186900999`.

LAUNDER, B.E. and SPALDING, D.B. (1974). "The numerical computation of turbulent flows". *Computer Methods in Applied Mechanics and Engineering*, **3(2)**, 269–289.

LAWAL, K.A., CRAWSHAW, J.P., BOEK, E.S. and VESOVIC, V. (2012). "Experimental Investigation of Asphaltene Deposition in Capillary Flow". *Energy & Fuels*, **26(4)**, 2145–2153. URL `https://pubs.acs.org/doi/10.1021/ef201874m`.

MAGNINI, M. and MATAR, O.K. (2019). "Fundamental study of wax deposition in crude oil flows in a pipeline via interface-resolved numerical simulations". *Ind. Eng. Chem. Res.*, **58**, 21797–21816.

MARON, S.H. and PIERCE, P.E. (1956). "Application of ree-eyring generalized flow theory to suspensions of spherical particles". *Journal of Colloid Science*, **11(1)**, 80–95.

MUNICCHI, F. and ICARDI, M. (2020). "Generalized multirate models for conjugate transfer in heterogeneous materials". *Physical Review Research*, **2(1)**, 013041. `1906.01316`, URL `http://arxiv.org/abs/1906.01316https://link.aps.org/doi/10.1103/PhysRevResearch.2.013041`.

NOTT, P.R. and BRADY, J.F. (1994). "Pressure-driven flow of suspensions: simulation and theory". *Journal of Fluid Mechanics*, **275(-1)**, 157. URL `http://www.journals.cambridge.org/abstract_S0022112094002326`.

RAMIREZ-JARAMILLO, E., LIRA-GALEANA, C. and MANERO, O. (2001). "Numerical simulation of wax deposition in oil pipeline systems". *Petrol. Sci. Technol.*, **19**, 143–156.

RAMIREZ-JARAMILLO, E., LIRA-GALEANA, C. and MANERO, O. (2004). "Modelling wax deposition in pipelines". *Petrol. Sci. Technol.*, **22**, 821–871.

ROUSSEL N, ROY RL, C.P. (2004). "hixotropy modelling at local and macroscopic scales". *Non-Newton Fluid Mech*, **117(85)**.

SILERI, D., SAHU, K.C. and MATAR, O.K. (2011). "Two-fluid pressure-driven channel flow with wall deposition and ageing effects". *Eng Math*, **71**, 109–130.

SINGH, A., PANACHAROENSAWAD, E. and SARICA, C. (2017). "A mini pilot-scale flow loop experimental study of turbulent flow wax deposition by using a natural gas condensate". *Energy Fuels*, **31**, 2457.

SINGH, P., VENKATESAN, R., FOGLER, H.S. and NAGARAJAN, N. (2001). "Morphological evolution of thick wax deposits during aging". *AIChE J.*, **47**, 6–18.

SINGH, P., VENKATESAN, R., FOGLER, H.S. and NAGARAJAN, N. (2000). "Formation and aging of incipient thin film wax-oil gels". *AIChE Journal*, **46(5)**, 1059–1074. `https://aiche.onlinelibrary.wiley.com/doi/pdf/10.1002/aic.690460517`, URL `https://aiche.onlinelibrary.wiley.com/doi/abs/10.1002/aic.690460517`.

SOLAIMANY NAZAR, A.R., DABIR, B. and ISLAM, M.R. (2005). "Experimental and mathematical modeling of wax deposition and propagation in pipes transporting crude oil". *Energy Sources*, **27**, 185–207.

SVENDSEN, J.A. (1993). "Mathematical modeling of wax deposition in oil pipeline systems". *AIChE Journal*, **39(8)**, 1377–1388.